
The new Digital Elevation Model data set from the Shuttle Radar Topography Mission : Hydrogeomorphological applications in the Ohrid region (Albania, Greece and Macedonia)

Christian DEPRAETERE* Serge RIAZANOFF**

*Laboratoire d'étude des Transferts en Hydrologie et Environnement (LTHE) BP 53 38041 Grenoble cedex 9 FRANCE

** GAEL Consultant, Cité Descartes 18, rue Albert Einstein 77420 Champs-sur-Marne, FRANCE

Abstract:

A new Digital Elevation Model data set (DEM) from the Shuttle Radar Topography Mission (SRTM) at 3 arc-sec resolution has become available at no cost for the Balkanic region from november 2003. SRTM consists of a specially modified radar system that flew onboard the Space Shuttle Endeavour in the year 2000.

This paper presents the results of a first evaluation of the suitability of the DEM/SRTM for hydrogeomorphological applications for the Balkans. The study is carried out on the Drim catchment basin including the Ohrid and Prespa lakes (Macedonia, Albania and Greece).

One major benefit of the DEM/SRTM data base is that the DEM is homogeneous over the entire Balkans. This should facilitate transferability of local results to other regions. The study investigates first the specific limitations of the data sets such as artefacts resulting from the speckle effect generated by the radar. These artefacts are responsible for erroneous results for slope and drainage lines with gradient below 6%. On steeper slopes, river networks and watersheds are comparable to what can be seen on maps at 1/100.000 scale. This result suggests that the basic hydrogeomorphological operations required for hydrological applications (computation of slope gradients, river network delineation, catchment basin partition) are satisfactory for most areas of balkanic region apart from relatively flat plains.

The second part of the paper evaluates a new method dedicated to massif extraction instead of catchment basin partition, which has been already largely explored and implemented in hydrological sciences. Massifs can be considered as the counterpart of catchment basins if one consider the land surface upside down. Nevertheless, the two systems of land partition are not symmetrical. The topological properties of catchment basins and related talweg networks are determined by hydrological processes responsible for the carving of valleys. On the other hand, massifs and related crest lines appear to be more closely associated with the geological structure including lithology and tectonic. In the Ohrid region, the massifs are mainly mountain ranges or plateaux with specific "geomorphometric signatures" symptomatic of potential differences in transfer and production functions. A method is proposed for automatic detection of massif with karstic structure. Combined with catchment basin partitions, massif partitions of the land surface appear to be a useful source of information for automatic delineation of homogenous hydrological units to be used in distributed hydrological models.

The DEM/SRTM data base offers the basic capabilities for most applications in hydrology all over the world. In the specific context of the Balkans where no dense DEM were available before, these DEM product may constitute a major breakthrough in a near future for hydrological modelling and environmental GIS.

Key words: DEM, Geomorphometry, Hydrology, Massif, landform signature, Karst, Balkans, Drim catchment, Ohrid.

The new Digital Elevation Model data set from the Shuttle Radar Topography Mission : Hydrogeomorphological applications on the Ohrid region (Albania, Greece and Macedonia)

Christian DEPRAETERE Serge RIAZANOFF***

**Laboratoire d'étude des Transferts en Hydrologie et Environnement (LTHE) BP 53 38041 Grenoble cedex 9 FRANCE*

*** GAEL Consultant, Cité Descartes 18, rue Albert Einstein 77420 Champs-sur-Marne, FRANCE*

INTRODUCTION

Digital Elevation Model (DEM) have become a customary element for physically distributed hydrological model. The major drawback and limitation in their usage were their lack of “off the shelves” availability in many countries and their heterogeneity.

The new generation of DEM from the Shuttle Radar Topography Mission (SRTM) at 3 arc-sec resolution is gradually becoming available for the entire Earth (for the entire balkanic region since november 2003). The first objective is to evaluate the artefacts and the resulting limitation of this DEM for usual application in hydrology.

After a general introduction on geomorphometry, a method is presented for automatic partition of the land surface into massifs and applied on the Ohrid region (Albania, Macedonia and Greece). The massif are the counterpart of catchment basins in the “anti relief”. The algorithm of massif partition has some analogy with watershed extraction technique from DEM but with specific adaptations. The concern with massifs compared to watersheds is due to their close relation with the geological basement especially in the balkanic context. This partition is then complementary of the catchment basin partition which is more process orientated. In a second step starting from the massifs, several landform criteria are tested to discriminate the “geomorphometrical signature” of specific geological bases such as karst.

These two steps of partition and classification of the land surface exemplify specific geomorphometry. The final output is a pre classification of the land surface into lithologically contrasting massifs supposedly related to past and present hydrological processes. It ease the work of land classification necessary to distribute the transfert and production functions over large areas such as the balkanic peninsula for which no large scale and homogeneous geological maps are available. It provides also an objective alternative to the information given by geological map which are barely suitable for hydrological needs.

1./ The new DEM/SRTM and specific artefacts :

To use the DEM/SRTM some background information is required, such as sources and qualities of the given DEM. The Shuttle Radar Topography Mission (Werner 2001) obtained elevation data (Rabus et al. 2003) on a near-global scale to generate the most complete high-resolution digital topographic database of Earth. SRTM consisted of a specially modified radar system that flew onboard the Space Shuttle Endeavour during an 11-day mission in February of 2000. Processing the SRTM data took two years to complete.

The SRTM instrument¹ consisted of the Spaceborne Imaging Radar-C² (SIR-C) hardware set modified with a Space Station-derived mast and additional antennae to form an interferometer with a 60 meter long baseline (Farr and Kobrick, 2000). SRTM radar echo data were processed into elevation information in a systematic fashion using the SRTM Ground Data Processing System (GDPS) supercomputer system at the Jet Propulsion Laboratory.

Vegetation canopy and building affect the radar echo. Therefore, SRTM data is by definition not a digital terrain model (DTM elevation of the earth surface) but a digital elevation model (DEM).

The specifications of errors on this DEM/SRTM are given in table1 :

Table 1: Specifications of errors on DEM/SRTM

Errors	absolute	Relative
Horizontal	±20m 90% circular	±15m 90% circular
Vertical	±16m 90% vertical	±6m 90% vertical

The DEM made from radar data shows specific artefacts :

- ❑ Speckling artefact : randomly distributed elevation spikes are clearly identified over areas of low relief but also affect steepest areas.
- ❑ Gaps in the data : infrequent gaps in data coverage requires filling methods to cope with missing elevation (interpolation or data from other DEM/DTM).

These two types of artefact are observed on the Ohrid region as shown on figure 1. The granulation due to the speckle is visible on lakes and flat zones. Gaps are mostly on lakes but also on steep sides of mountains.

The variogram of speckling over the Ohrid lake is characterized by a range of 6 arc-seconds (figure 2). Any sub-set resampled at a resolution over 6 arc-seconds will avoid the problem of speckle.

2./ Applications of partitioning methods for watersheds and massif extractions:

2.1./ Review on geomorphometry :

This review tries to summarize the standard uses of DEM for landforms classification. With Evans (1972), specific and general geomorphometry has to be distinguished (figure 3) : specific geomorphometry assumes a definition of specific landforms that will be considered before they are analysed with ad hoc criteria; conversely, general geomorphometry starts with an overall analysis of the land surface that will serve for further identification of homogenous morphological units.

¹ SRTM is an international project spearheaded by the National Imagery and Mapping Agency (NIMA) and the National Aeronautics and Space Administration (NASA). The SRTM data resulted from a collaborative effort by the NASA and NIMA, as well as the participation of the German and Italian space agencies, to generate a near-global digital elevation model (DEM) of the Earth using radar interferometry.

² NASA is also processing the C-band radar image data and plans to make the data available to the public around the end of 2003. The X-band is being processed by the German Aerospace Center, DLR and the C-band is being processed by NASA. C-band and X-band are the different wavelengths that were used to collect the data.

The rationale of this paper focuses on the specific geomorphometry (figure 4) approach with two types of predefined morphological unit : catchment basins and massifs. The choice of catchment basin is obvious for hydrology as a functional unit. Massifs are not so commonly used despite the fact that they constitute the logical complementary element of the previous. They are also suitable for morpho-structural partition of the land surface as we will see in this paper. The objective is less ambitious than some other works in automatic terrain analysis (cf. Argialas, 1995) and will be limited to identification of specific geomorphometric signature of karst massifs. This choice is partly due to the importance and the extent of karst in the balkanic region and their peculiar hydrologic functioning.

2.2./ The method of massif partitioning :

Landform characteristics depicted by Digital Elevation Modelling techniques appears to be a very versatile source of understanding for hydrological processes previously illustrated for instance in the work of Kirkby and Beven (soils potential saturation index SPSI), Rodriguez and Iturbide (geomorphological hydrograph). Hydrogeomorphological applications of DEM/SRTM have already been evaluated on some regions (Falorni et al. 2003).

2.2.1/ Watershed versus massif partitions of the land surface :

Two sets of methods will be applied to the DEM, one for watershed and river network extraction, the other for massif and crest line extraction. Both methods are actually variants of the same algorithms as we will see in this chapter.

The method for watershed and river network extraction is commonly used for hydrologically dedicated GIS and distributed hydrological modelling (Jensen 1985, Band 1986, 1989, Jenson & Domingue 1988, Tarboton et al. 1994). The basic algorithm is based on the steepest descent principle and pit removal for delineation of surface water flow paths (Hutchinson, 1989). Distinction between river network (concentrated flow) and other flow paths corresponding to hillslopes (non concentrated flow) is usually based on assumption that over a certain area for the drained surface the water becomes concentrated into a valley bottom and initiates a river (Depraetere, 1990). After definition of river networks, catchment basins can be codified and classified according to various types of hierarchical methods (Depraetere & Moniod 1991). Examples of watersheds and river networks delineation from DEM/SRTM over the Ohrid region are given in figure 5.

Conversely, massif extraction and related crest network are less commonly used. This paper will emphasize this aspect which seems to have been neglected so far. Massifs can not be considered as an objective hydrological unit comparable to catchment basins but they constitute morpho-structural units that may have generally specific and homogenous landform signature.

Massif partitioning of mountainous regions could be seen as a rather intuitive perception of the land. This fact is exemplified on the tetradrachm coin of the region of Ephesus in Asia Minor dating back from the fourth century BC (figure 6a). The pattern on the reverse side of this coin remained quite enigmatic until it was compared with the relief map of the same region (Harvey, 1980) as it is shown on figure 6b.

Amongst various possible operational definitions of massif, the most appropriate one is to consider at the initial stage that it encompasses all the points converging towards a summit in term of steepest ascents. The steepest ascent is similar to the steepest descent if one considers the elevation surface upside down (we note that a massif is in fact a kind of “anti catchment basin” related to the “anti relief”). After definition of initial massifs, the second phase is to merge them step by step into a larger massif subject to certain conditions related to differences of summit elevation and connection of saddle points (“stepwise merging”).

The two methods of catchment basins versus massifs partitions are summarised in table 2:

Table 2: General characteristics of catchment basins versus massifs partitioning of DEM

	Basic direction	“Pit” removal	Convergence point	Main path lines	Classification
Catchment basin	Steepest descent	Yes*	Outlet	Talweg (river)	Various**
Massif	Steepest ascent	No	Summit	Crest	Stepwise merging

* pit removal is compulsory for catchment basin extraction to get rid of spurious (artificial) pits.

** usual Horton, Shreve, ... ordering principles or other more appropriate topological coding of catchments and talwegs.

2.2.1/ Methodology of massif partitions :

For convenience, the method exposed in this chapter will be called MAPAM for Massif Partitioning and Merging. The final output is an optimized partition of the land surface into massifs with a significant perched compared to their surrounding lowlands.

The first phase of MAPAM is to define the “initial massifs”. Initial massifs are related to only one summit. Lets assume that the steepest ascent lines converging toward a summit have been computed. It is then possible to define land units that are related to the same summit by the steepest ascent lines. Each portion is then consider as the set of initial massifs, each of which contains only one summit by definition.

Two variables must be associated with each massif for further calculation :

- The elevation of the summit Z_{\max}
- The elevation of the highest point at the rim of the massif. This point correspond to the highest saddle point Z_{hsd} . The location of the highest saddle point is also relevant to define the connection between the massif and one of its neighbours.

At the end of the initial step (called Step 0), a set of m massifs is then defined with their related variables $Z_{\max}(1)$ to $Z_{\max}(m)$ and $Z_{\text{hsd}}(1)$ to $Z_{\text{hsd}}(m)$. counterpart

The second phase of MAPAM will initiate a step by step merging from the initial massifs. The massif i is merged with the massif j subject to the following conditions :

- Massif i is connected to massif j via the $Z_{\text{hsp}}(i)$ point (“highest saddle point connection”),
- The highest elevation of massif j is greater than its counterpart for massif i ($Z_{\max}(j) > Z_{\max}(i)$).

This merging rule is repeated at each step until the entire land surface is integrated into the same massif (the number of merging steps depends of the complexity of landforms).

The phase one and two of MAPAM are exemplified on the Gorenichka massif located at the north of the Ohrid lake (figure 7). At the initial step (Step 0), the region is partitioned into

69 small massifs associated with the same number of summits. In this case, the entire massif is aggregated after 2 steps of merging. Beyond step 2, the Gorenichka massif is merged with one of its neighbours.

The final stage of MAPAM requires the definition of criteria to decide which step of merging is the more convenient for a specific massif. Two indices of massifs landforms will be introduced for this purpose:

- index of massif pertinence I_{massif} :

$$I_{\text{massif}} = (Z_{\text{max}} - Z_{\text{hsp}}) / (Z_{\text{max}} - Z_{\text{min}}) \quad I_{\text{massif}} \in [0..1[$$

with Z_{min} the minimum elevation at the rim of the massif
 Z_{max} the maximum elevation
 Z_{hsp} the elevation of highest saddle point at the rim of the massif

When this index tends to 1, it means that the elevation of the highest saddle point is close to the minimum elevation and it reflects that the massif is clearly topographical disconnected from its neighbours.

- index of global relative elevation I_{ih} (hypsothetic integral) :

$$I_{\text{ih}} = \left(\sum_{i=1}^n (Z_i - Z_{\text{min}}) / (Z_{\text{max}} - Z_{\text{min}}) \right) / n \quad I_{\text{ih}} \in [0..1[$$

Z_i elevation point i , massif with n elevation points
 Z_{hsp} the elevation of highest saddle point at the rim of the massif

When this index tends to 1, the massif could be assimilated to a plateau. Conversely when it tends to 0, the massif could be seen as a plain with small high points dominating the plain.

For a given group of massifs, the best step of merging occurs when the I_{massif} index is maximum. Considering the previous example on the Gorenichka massif, the optimum is obtained at step 2 (figure 8). The further step gives a lower value for this index indicating a less significant grouping of this massif with its neighbours. We note that the maximum value of the hypsothetic integral I_{ih} also occurs at step 2. This suggests that the plateau like shape of this massif is most sensitive at this step.

The three stages of MAPAM processing are listed below :

- Stage 1: extraction of initial massifs and computation of their Z_{max} to Z_{hsp} characteristics.
- Stage 2: stepwise conditional merging of massifs. At the end of it, the complete set of data includes all the massifs defined at each step including the initial massifs. The two indices of massifs landforms I_{massif} and I_{ih} are computed for each massif.
- Stage 3: definition of the optimal massif partition. The optimal partition for a given massif corresponds to the step where the index I_{massif} is maximum. For an overall partition, a minimum value of the index I_{massif} has to be defined ($I_{\text{minmassif}}$). The resulting selected massifs ($I_{\text{massif}} > I_{\text{minmassif}}$) include all topographically well defined massifs regardless of the step at which they have been defined. This “optimal” set may include embedded elements and is no longer a partition of the land surface (the same point may belong to several massif). The embedded massifs must be either eliminated or spatially partitioned.

2.3./ Application of massif partitioning over the Ohrid region :

The general landform characteristics of the Ohrid region need to be defined before application of the MAPAM. Specific pre processing of the DEM/SRTM is also described in this chapter.

2.3.1./ A basic regional model of landform patterns based on directional variograms:

The balkans are well-known for their paving of mountains and depression. The Ohrid region appears as a representative case of this type of compartmented landscape reflecting the influence of the geological structure. The directional variograms of the DEM over the Ohrid region could give us an insight into the organisation of these main landform features (figure 9). The major contrast appears between the WSW-ENE axis and its orthogonal direction NNW-SSE. The latter direction is parallel to the main ridges and valley of the region and its variogram is related to a range (R1) of 18 km with a sill of 270000 (S1=519 meters) and a gentle trend at 18 km onward. The orthogonal direction clearly depicts the dominant and regular ridge and valley structure on its variogram with a range (R2) of 15 km and a sill of 320000 (S2=566 meters). The ranges of the variograms represent the average spacing between valley and ridges while the sills give an order of magnitude for amplitude of elevation between them. These figures are broadly consistent with the land pattern of the region (figure 10).

This provides a prognosis for the size of the major massifs. The average size of these massifs could be estimated from the ranges of the two orthogonal axes : about 1000 km² ((2xR1)x(2xR2)). The sills are related to amplitude of elevation between crest lines and foothills in a more complex way. Depending of the shape of the massif, the real amplitude defined as the difference between max and min elevation should be 2 or 4 times the average value given by the sills of the two orthogonal axis ((S1+S2)/2), in this case between 1000 and 2000 meters.

The directional variogram appears as a simple method to pinpoint the main characteristics of a complex land surface. It provides at least a regional model before using more elaborate methods. The method of massif partitioning described previously will allow us to analyse the variability of local landforms in terms of scale, shape and relief, and compare them with what has been deduced from this straightforward regional model.

2.3.2./ Specific pre-processing of the DEM :

Specific pre-processing of the DEM has to be made on the DEM/SRTM before application of the MAPAM process. The Ohrid and Prespa lakes were delimited on the DEM partly from external information (maps) and partly by taking into account the extension of area with dominant speckle effect (see figure 1).

Apart from the area corresponding to water bodies, it should be noted that the speckle effect is directly responsible for irrelevant erroneous results over areas with slope gradient less than 6%. In these areas, both steepest descent and ascent computing will produce erratic and twisty talweg and crest lines completely inaccurate compared to reality. These relatively flat zones mostly correspond to plains surrounding the lakes and the plain of Korçë (see figure 5). They correspond on the whole to recent alluvial deposit from rivers or lakes. They may

encompass also some specific landforms at the foot of massifs (alluvial fans, ...). These areas will not be taken into account in the MAPAM process for both reasons : inaccurate landform definition and mainly alluvial deposits independent of the massifs structure.

2.3.3./ Applications of the MAPAM process in the Ohrid region:

The automatic stepwise merging of massif has been applied to the Ohrid region from step 0 up to step 8. Beyond step 8, all the region is integrated into one massif. The average size of massifs range from 1.72 km² at step 0 to 5775 km² at step 8 (figure 11).

General trends are observed on the two landform indices. The average massif index I_{massif} increases steadily from 0.21 at step 0 to 0.8 at step 8 while the average hypsometric index I_{hi} integral decrease slowly from 0.49 at step 0 to 0.4 at step 8. The higher the step better the definition of the massifs (increase of I_{massif}) and the smaller the plateau landform appearance (decrease of I_{hi}). A threshold is sensitive at step 5 corresponding to what has been observed in the regional model. Above this step, the hypsometric index is stabilized at a value of 0.4 and the massif index is not increasing at the same rate. We assume that the merging process of massif is not anymore noteworthy in terms of the landscape unit beyond step 5.

This global overview is just indicative of the step to which the massif merging process must be considered. The intricate map of figure 12 shows the resulting hierarchical pattern of massifs and suggest theirs relation with the talweg network and finally the faulting system.

The massif index will be used to select the most significant massif whatever the step considered (figure 13 with $I_{\text{massif}} > 0.65$). The main massifs surrounding the lakes of Prespa and Ohrid correspond more or less to homogeneous geological unit (figure 14). The relation is more intricate in the west and north-west of the region.

It may be noted that we don't have proper homogeneous lithological maps covering the entire region at the moment. Therefore, it is difficult to make a precise prognosis of the lithology from the geological map used in this paper. This is a disadvantage for the validation of the results but it also illustrates the difficulty of finding homogeneous suitable information on the geological base relevant for hydrology.

3./ Geomorphometrical signature of massifs :

The objective is to explore which type of geomorphometrical signature is the most appropriate to differentiate the geological setting of massifs as given by MAPAM, especially the karstic ones from the others. For this purpose, a set of massifs is selected to test the discrimination capability of various geomorphometrical criteria. The calibration set of massifs corresponds to those that are geologically well defined (see massif numbers for this calibration set in figure 14). The other massifs will be used in the corroboration phase. The calibration set includes various type of bedrock and morphology : high Karst (49), low karsts (33, 34 and 37), partly karst (57), high mountain with fluvial landform (53), low mountain with fluvial landform (46 and 56), hilly landforms (40 and 41).

3.1./ Geomorphological signature criteria for recognition of karst massif :

Many geomorphometrical or geostatistical criteria can be used to differentiate landform signatures over a predefined land unit. There are presented and discussed in various

publications such as Evans (1972,1987), Depraetere (1984, 1992), Nogami (1985), Pike and Dikau (1995), Wilson and Gallant (2000). From these authors, few geomorphometrical parameters are shown in table 3 :

Table 3 : common geomorphometrical parameters computed from DEM

Geomorphometrical Parameters	Comments	Abbrev.
Elevation	Potential energy, climatic and vegetation control	Raele
Slope gradient	Overland and subsurface flow velocity runoff, land uses	Sgrad
Slope aspect	Solar insolation, climatic and vegetation control	Saspe
Plan convexity	Diverging or converging of flows (talweg/crest)	Cplan
Profile convexity	Acceleration or deceleration of flows (concave/convex)	Cprof
Transverse convexity	Embedment of valley, dominance of interfluve	Ctran
Quadratic mean curvature	Global curvature of landforms	CUqm
Total curvature (laplacian)	Global curvature with concave or convex classes.	CUtot

Methods of descriptive statistics (mean, standard deviation, ...) applied to geomorphometric measurements over massif are unable to differentiate their specific signature related to their geological types. Other criteria such as the hypsometric integral (Ih) or variogram are also inadequate for this purpose.

The difference of signature is mainly related to the concave/convex properties of landforms especially around talweg and crest lines. To quantify this difference, plan and profile convexities will be considered in this explorative phase. The plan convexity is useful to distinguish talweg from crest: talweg have negative values, crest have positive values. The profile convexity defines concave versus convex hillslopes : negative values correspond to concave landform (decrease of slope gradient downhill), positive landform correspond to convex landform (increase of slope gradient downhill). The combination of these two types of convexities makes a set of landforms as defined by Ruhe (1975) and illustrated on figure 15.

A statistical approach to real landforms of the Ruhe classification can be taken by making a scatter plot of plan convexity versus profile convexity. Applied on the massifs of the Ohrid region, the relationship between the plan convexities and the average of profile convexities (Cplan x Cprof) is symmetrical as it is shown on the example of the karst massif of Galichitza (Figure 16a). Relationship between both convexities are more or less the same on valley and ridge. This result suggests that the general architecture of landforms in the scope of the adapted classification of Ruhe is dominantly a triptych formed by concave (*Concav Concav* (--)), neutral (*Neutral Neutral* (00)) and convex (*Convex Convex* (++)) landforms.

Considering now the logarithm value of the plan convexity Log(Cplan), the relation of Log(Cplan) with profile convexity becomes linear (figure 16b) on the entire range of values including talweg and crest. This linear “global” relation is given in (1) and is summarized by two parameters a_{global} and b_{global} :

$$(1) \text{ Global (Log(Cplan) x Cprof)} : Cprof = a_{\text{global}} \text{Log(Cplan)} + b_{\text{global}}$$

This global statistical relation (Log(Cplan)x Cprof) can be adjusted separately to talweg (Cplan<0) and crest (Cplan>0). Following the same logic, two specific models are defined in (2) and (3) :

$$(2) \text{ Talweg } (\text{Log}(\text{Cplan}) \times \text{Cprof})) : \text{Cprof} = - (a_{\text{talweg}} \text{Log}(-\text{Cplan}) + b_{\text{talweg}})$$

$$(3) \text{ Crest } (\text{Log}(\text{Cplan}) \times \text{Cprof})) : \text{Cprof} = a_{\text{crest}} \text{Log}(\text{Cplan}) + b_{\text{crest}}$$

It has to be noted that the “talweg” model as given in (2) has been adapted to be comparable with the “crest” model. Figure 16c is related to the two specific models for the Galichitza massif. It confirms that the relationship between the two types of convexity is closely similar for both talweg and crest on this karst massif.

The parameters a_{global} , a_{talweg} and a_{crest} will be use as synthetic criteria of the geomorphometric signature of the calibration set of massifs defined previously.

Table 4 : main characteristics of a calibration set of massifs and values of geomorphometrical criteria to identify the karsts.

Name of the massif	Code	Geological Type (from maps)	Planimetry		Location		Relief			geomorphometrical signatures (from DEM)		
			Surface km ²	Perimeter km	Longit.	Latit.	Zmax m	Amp m	Ih %	aGlobal	aCrest	aTalweg
Suva Gora	34	Karst	159,4	85,5	20,999	40,752	1481	652	54,6	42,5	54,3	27,3
Galichitza Planina	49	Karst	591,0	217,5	20,865	40,964	2280	1593	61,8	50,3	51,6	49,7
Triklarion Oros	33	Karst	146,3	84,3	21,084	40,673	1741	898	62,5	53,8	53,6	51,1
Koresta	37	Karst	209,7	79,7	21,098	40,589	1784	1111	64,6	51,6	59,9	52,0
Jablanica Planina	57	Partly karst(?)	916,7	229,7	20,473	41,297	2238	2023	54,1	61,0	59,4	58,7
Maja e Buzmadhit	40	Hilly	300,4	109,7	20,598	40,643	1628	1097	41,8	62,5	70,9	59,1
Morava	41	Hilly	364,3	173,5	20,817	40,575	1860	1040	62,4	58,9	59,7	60,5
Stogovo Planina	46	Non karst	505,5	165,3	20,67	41,395	2257	1707	57,0	63,7	65,9	68,8
Plakenska Planina	56	Non karst	905,4	343,6	21,005	41,273	1987	1371	69,7	63,6	64,9	69,5
Baba Planina	53	Non karst	819,8	214,1	21,187	40,848	2592	1971	61,9	69,2	76,9	73,1

Zmax : max elevation. Amp : range of elevation (Zmax-Zmin). Ih : hypsometric integral (potential energy)

Compared to geological types as identified on maps, the parameter a_{talweg} is the most appropriate to discriminate the karst massifs from the others while the parameter a_{crest} appears to be less significant. Just by considering this result, the following classification of landform signature according to the parameter a_{talweg} is proposed :

- ❑ $a_{\text{talweg}} < 55$: likely to be karst (massifs 33, 34, 37 and 49),
- ❑ $55 < a_{\text{talweg}} < 64$: likely to be partly karst (massif 57) or hilly (massifs 40 and 41),
- ❑ $a_{\text{talweg}} > 64$: likely to be fluvial landforms (massifs 46, 53 and 56).

The most contrasting massifs in terms of geomorphometrical signature (3 parameters) are the Baba Planina (#53) and the Suva Gora (#34). They are also the two massifs with sharp lithological differentiation:

- ❑ The Baba planina massif is a high massif of granite and metamorphic rocks,
- ❑ The Suva Gora is entirely karstic with large and rounded valleys.

3.2./ Corroboration of the criteria :

The other massifs have been use in the corroboration phase (figure 17). For this set, the parameter a_{talweg} alonen is not sufficient to differentiate karst from other massifs : for instance the massif Bel Kamen #31 is classified as karst while it is not, the massif Precna #22 is classified as non-karst while it is a karst. A scoring factor K is then introduced to cope with ambiguous geomorphometrical signature.

The scoring factor K built for identification of karst is defined as follows :

$$K = K_{tal} + K_{ave} + K_{min} \quad (K \in [-3..3])$$

With $K_{tal} = -1$ if $a_{Talweg} > 62$, $K_{tal} = 1$ if $a_{Talweg} < 55$ ($K_{tal} \in [-1,0,1]$)
With $K_{ave} = -1$ if $((a_{global} + a_{Crest} + a_{Talweg})/3) > 62$, $K_{ave} = 1$ if $((a_{global} + a_{Crest} + a_{Talweg})/3) < 55$ ($K_{ave} \in [-1,0,1]$)
With $K_{min} = -1$ if $(\min(a_{Crest}, a_{Talweg})) > 62$, $K_{min} = 1$ if $(\min(a_{Crest}, a_{Talweg})) < 55$ ($K_{min} \in [-1,0,1]$)

The K scoring factor ranges from -3 (fully non-karst signature) to 3 (fully karst signature). With this geomorphometrical criterion, several massifs are recognized as fully non-karst while only the small massif of Udha Male #21 has a fully karst signature. Several massifs have elements of a karst signature. Amongst them, the massifs of Bel Kamen #31 and Precna #22 remains ambiguous and give reason for detailed comments. The Bel Kamen with a K factor of 2 has the same geological base with its surrounding massifs which are all classified as non-karst. This inconsistency might be explained by the burial of the piedmont by recent alluvial deposits (large alluvial fans from the Baba Planina massif, alluvial plain in the north). In consequence, the original talweg landforms may be partly hidden. The fact that the crest parameter a_{Crest} is consistent with a non-karst signature weighs in favour of this hypothesis. The Precna massif constitutes the opposite case of misclassified landforms. The landform of this karst looks similar to the karst of Suva Gora #34. Its crest parameter is typical of karst ($a_{Crest}=18,9$) but the talweg parameter is unusually high for a karst ($a_{talweg}=62,7$). One possible explanation involves a pflooding of the piedmont part of the massif by the water of Prespa lake which was at a lower level in the past.

These two cases illustrate the limits of the method without dismissing it. Both misclassifications are linked to very local conditions if we consider the hypotheses put forward to explain them. One interesting point with these two examples is that the crest parameter seems to be more “robust” in terms of proper identification of ambiguous cases. This finding is consistent with the fact that crests are less affected by local recent evolution (change in base level, alluvial deposit, neotectonic) than talweg. The table 4 sums up the prognosis of karstic landform for the entire region.

The proposed method geomorphometric of signature discrimination based on the cross combination of plan and profile convexities applied on talweg and crest of massifs offers promising capabilities for automated landform survey. For convenience, it may be called the C2SIGN method. This exploratory work combining MAPAM and C2SIGN on a small region requires validation on larger areas with other partition techniques or classification methods (see the example of massif partitioning on a part of Balkan in figure 18).

Table 4: Karst geomorphometrical signature on the corroboration set of massifs

Name of the massif	Code	Geological Type (from maps)	Surface km ²	geomorphometrical signatures of karst (scoring from DEM)						
				a _{Global} (1)	a _{Crest} (2)	a _{Talweg} (3)	K _{tal}	K _{ave}	K _{min}	Score K
Udha Male	21	Karst	29,3	46,7	36,7	46,0	1	1	1	3
Gorenichka	23	Karst	32,3	58,0	85,6	36,8	1	0	1	2
Bel Kamen	31	Non_Karst	99,7	60,1	70,8	49,5	1	0	1	2
Mali i Gjalicës	28	Karst	69,0	61,0	71,6	49,9	1	0	1	2
Bukovi	26	Karst	60,7	53,2	51,2	59,1	0	1	1	2
Suva Gora	45	Limestones(?)	463,2	58,2	54,5	55,5	0	0	1	1
?	30	?	86,6	54,8	36,4	62,5	-1	1	1	1
Precna	22	Karst	29,0	43,2	18,9	62,7	-1	1	1	1
Mali i Shenjt	42	Limestones(?)	451,6	62,8	61,1	56,7	0	0	0	0
?	24	?	32,7	56,7	68,0	57,4	0	0	0	0
Mal Korab	55	Non_Karst	868,7	61,0	59,4	58,7	0	0	0	0
Maja e Dhogzit	58	Non_Karst	975,0	61,0	60,4	61,2	0	0	0	0
Ostravica	52	Partly Karst	785,5	61,4	63,0	61,5	0	0	0	0
Bistra Planina	50	Non_Karst	627,0	59,0	52,5	67,2	-1	0	1	0
Mali Buzëmadhe	39	?	267,2	61,4	51,8	72,7	-1	0	1	0
Radika Planina	54	Non_Karst	857,6	63,9	54,1	80,4	-1	-1	1	-1
?	38	Partly-karst	215,4	66,0	69,3	63,7	-1	-1	-1	-3
Stara Buka	32	Non-Karst	104,8	66,0	69,3	63,7	-1	-1	-1	-3
Kazani	27	?	64,8	59,8	62,5	64,3	-1	-1	-1	-3
Bujeva Planina	48	Non_Karst	570,7	62,0	70,1	64,6	-1	-1	-1	-3
Mal Dejë	47	Non_Karst	544,7	64,3	69,4	65,5	-1	-1	-1	-3
Mal Zaloshnje	44	?	461,9	67,6	65,0	68,6	-1	-1	-1	-3
Pesjak	51	Non_Karst	639,0	67,4	74,9	70,2	-1	-1	-1	-3
Mal Allaman	43	?	460,6	68,3	73,3	71,8	-1	-1	-1	-3
Valamarë	59	Non_Karst	1956,1	67,4	72,1	72,4	-1	-1	-1	-3
Mali i Cukaravës	36	Non_Karst	206,7	73,7	82,4	74,3	-1	-1	-1	-3
?	25	Non_Karst	40,6	70,2	80,1	76,0	-1	-1	-1	-3
?	29	Non_Karst	75,2	78,1	88,0	76,1	-1	-1	-1	-3
Mal Munellë	35	Non_Karst	160,9	77,8	87,3	76,7	-1	-1	-1	-3

3.3/ Could we go further in a detailed analysis of landforms for hydrological application?

To answer this question, the geomorphological survey of the basin of Korçë (Albania) by Dufaure (2003) could be taken as an example of the close and complete relationships between geomorphology and hydrology approaches (figure 19a). He points out the *imbrications* of present and inherited landforms at the foothills of the Galichitza, Mali Thate and Morava massifs: the author tries to show a correspondence between the various generations of landforms (terraces, alluvial fans, canyons...), the paleoclimatology and the history of human occupation. The foothills of each massif at their point of contact with the depressions show sharp difference from one massifs to another. The alluvial fans coming from the Morava massifs have a very large extent compared to those of the Maja e Buzmadhit and reflect differing hydrological and sedimentary budget despite their geomorphometrical similarity as suggested in our paper. Figure 19b shows the detailed landforms that can be seen from the DEM/SRTM over the same region. The alluvial fans are partly visible on the foothills of the Morava massifs with the soil potential saturation index (SPSI Beven method). It suggests that the global definition of massif geomorphological signature presented in this paper could be conveniently implemented by more detailed analysis of specific landforms reflecting hydrological processes.

CONCLUSION :

This paper demonstrate the limitations and the potential of the newly available DEM/SRTM for analysis of geomorphometric signature. This approach is at the intersection of hydrology and geomorphology. It leads to a closer link between the landform signature and hydrological processes. Methods such as MAPAM combined with C2SIGN can help to overcome the recurrent problem of hydrologically pertinent and robust partition of the geological land surface for water resource modelling.

The new DEM/SRTM is rapidly becoming a new standard all over the world. Many other geomorphometrical measurements or criteria need to be investigated. For instance, the soil potential saturation index as a “synthetic” hydrological measurement is potentially for this approach. The implementation of more and more appropriate and detailed techniques on the large homogeneous DEM/SRTM in various contexts all over the world is likely to enlarge significantly the corpus of knowledge on relationships between geological base, landforms and hydrological processes.

References :

ARGIALAS, D. (1975): Toward structured-knowledge models for landform representation. Zeitschrift für Geomorphologie, Supplementband 101, pp.85-108, Gebrüder Borntraeger, Berlin, Stuttgart, december 1995.

BAND, L.E. (1986): Topographic partition of watersheds with digital elevation models. - Water Resources Research, 22: 15; Washington D.C..

BAND, L.E. (1989): A terrain-based watershed information system. - Hydrol. Processes, 3: 151-162; Chichester.

DEPRAETERE, C., (1984): Etudes géomorphométriques comparatives en Afrique du Sud : applications hydrologiques et géomorphologiques. Thèse de Troisième Cycle de Géographie, Université de Paris-Sorbonne, octobre 1984.

DEPRAETERE, C., (1990) : Seuillage du réseau hydrographique à partir de modèle numérique de terrain en fonction d'un critère de surface drainée. Troisièmes journées ULM (Utilités et Limites des Modèles), Laboratoire d'Hydrologie de l'ORSTOM, Montpellier, juin 1990, pp. 21-30.

DEPRAETERE C., MONIOD F., (1991) : Contributions des Modèles Numériques de Terrain à la simulation des écoulements dans un réseau hydrographique : exemple du bassin de Bras-David (Guadeloupe). Hydrologie Continentale, vol. 6, n°1, 1991, ORSTOM, Paris, pp. 29-53.

DEPRAETERE, C., (1992) : logiciel DEMIURGE version 2,0. Chaîne de production et de traitement des modèles numériques de terrain. Collection Logorstom, édition de l'ORSTOM, Paris, 1992.

DUFAURE, J.J. (2003): Regard sur les bassins intramontagnards sud-balkaniques : morphogenèse, milieux, sociétés. pp.49-60, Collection EDYTEM, Cahiers de Géographie n°1 2003, Dynamique et vulnérabilités des milieux montagnards méditerranéens et alpins, CISM, Université de Savoie, Le bourget du Lac, France.

EVANS, I.S. (1972): General geomorphometry, derivatives of altitudes, and descriptive statistics. In Chorley, R.J. (ed.): spatial analysis in geomorphology. Methuen, London.

EVANS (1987): The morphometry of specific landforms. In Gardiner, V. (Ed.): Int Geomorph. 1986 Part II, pp. 105-125. J. Wiley, Chichester.

FALORNI G., VIVONI E.R.(2), TELES V. (2) and BRAS R.L. (2003): Evaluating SRTM elevation products for hydrogeomorphological applications, Geophysical Research Abstracts, Vol. 5, 07436, 2003.

FARR, T.G., KOBICK M. (2000): Shuttle Radar Topography Mission produces a wealth of data, Amer. Geophys. Union Eos, v. 81, p. 583-585.

HUTCHINSON, M.F. (1989): A new procedure for gridding elevation and stream line data with automatic removal of spurious pits. - Journal of Hydrology:106: 211-232.

HARVEY, P.D.A. (1980): The history of topographical maps: symbols, pictures and survey. Thames and Hudson, Ltd. London.

JENSEN, S.K. (1985): Extracting topographic structure automated derivation of hydrologic basin characteristics from digital elevation model data. - Proc. Auto- Carto, 7: 301-310.

JENSEN, S.K. (1994): Application of hydrologic information automatically extracted from digital elevation models. - In: BEVEN, K.J. & MOORE, I.D. [Hrsg.]: Terrain analysis and distributed modelling in hydrology, 35-48; Chichester, N.Y., Brisbane.

JENSEN, S.K. & DOMINGUE, J.O. (1988): Extracting topographic structure from digital elevation data for geographic information system analysis. - Photogrammetric Engineering and Remote Sensing, 54 (11): 1593-1600; Falls Church.

KRCHO J., (2001): Modelling of georelief and its geometric structure using DTM – positional and numerical accuracy. Q111 publisher, 336pp. bi-lingual (English and Slovak) edition, first published 2001, Slovak State Cornelius University of Bratislava, Slovakia.

NOGAMI M., (1995) : Geomorphometric measures for digital elevation models. Zeitschrift für Geomorphologie, Supplementband 101, pp. 53-67, Gebrüder Borntraeger, Berlin, Stuttgart, december 1995.

PIKE, R.J., DIKAU R. (Ed.) (1995) : Advances in Geomorphometry. Zeitschrift für Geomorphologie, Supplementband 101, pp. 53-67, Gebrüder Borntraeger, Berlin, Stuttgart, december 1995.

RABUS, B., EINEDER M., ROTH A., BAMLER R. (2003):, The shuttle radar topography mission- a new class of digital elevation models acquired by spaceborne radar, Photogramm. Rem. Sens., v. 57, p. 241-262.

RUHE, R.V. (1975): Geomorphology. Boston Houghton Mifflin.

TARBOTON, D.G. & BRAS, R.L. & RODRÍGUEZ-ITURBE, I. (1994): On the extractions of channel networks from digital elevation data. - In: BEVEN, K.J. & MOORE, I.D. [Hrsg.]: Terrain analysis and distributed modelling in hydrology, 85-104; Chichester, N.Y., Brisbane.

WERNER, M. (2001): Shuttle Radar Topography Mission (SRTM), Mission overview, J. Telecom. (Frequenz), v. 55, p. 75-79.

WILSON, J.P., GALLANT, J.C. (Ed.) (2000) : Terrain analysis : principles and applications. JohnWiley & Sons, New York, Chichester, 2000.

Figure 1 :
Types of artefacts on the
DEM/SRTM in the region
of the Ohrid Lake

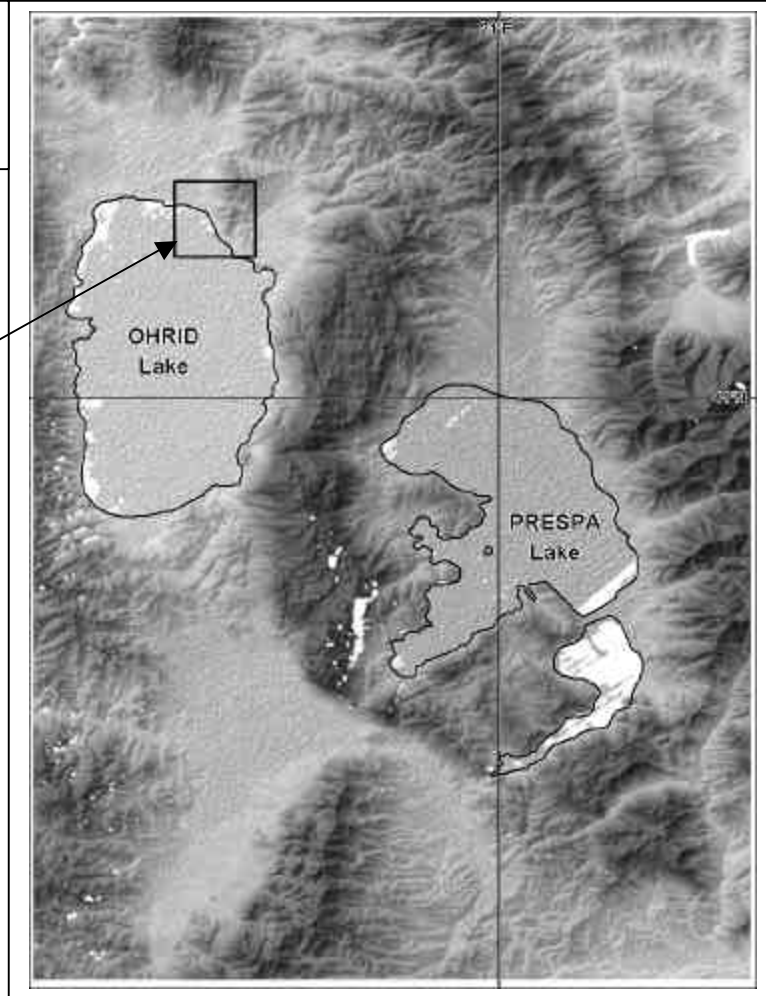
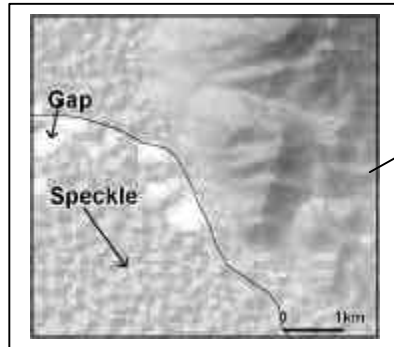


Figure 2 : Variogram of speckling over the Ohrid Lake

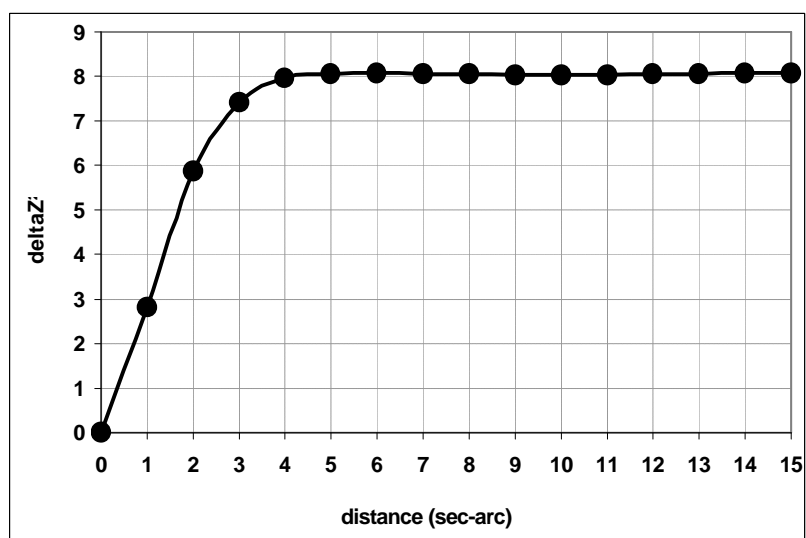


Figure 3 : specific versus general geomorphometry in terms of DEM processing steps

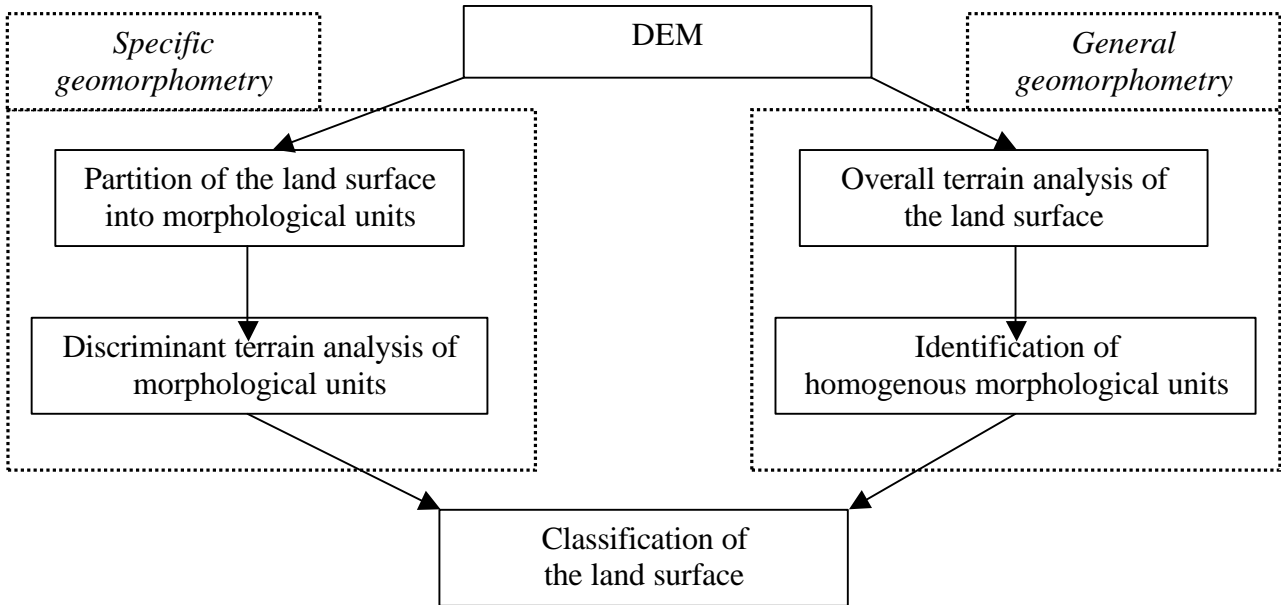


Figure 4 : specific geomorphometry for catchment basin and massif classifications

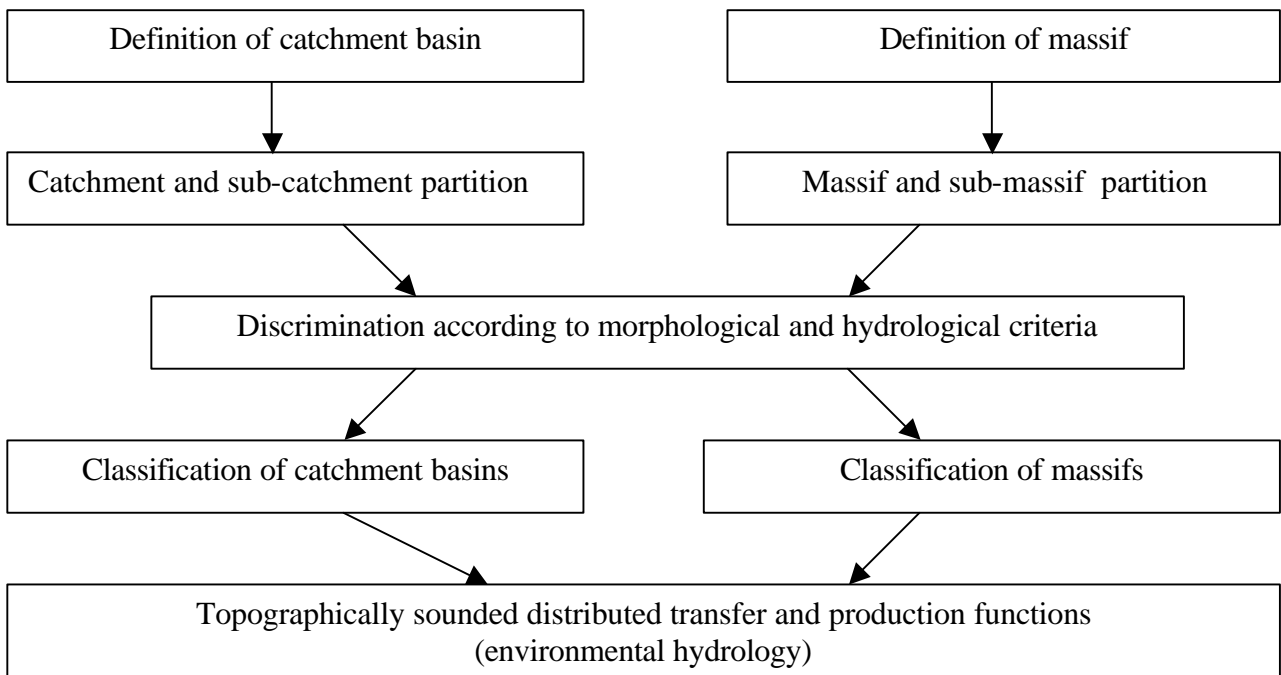
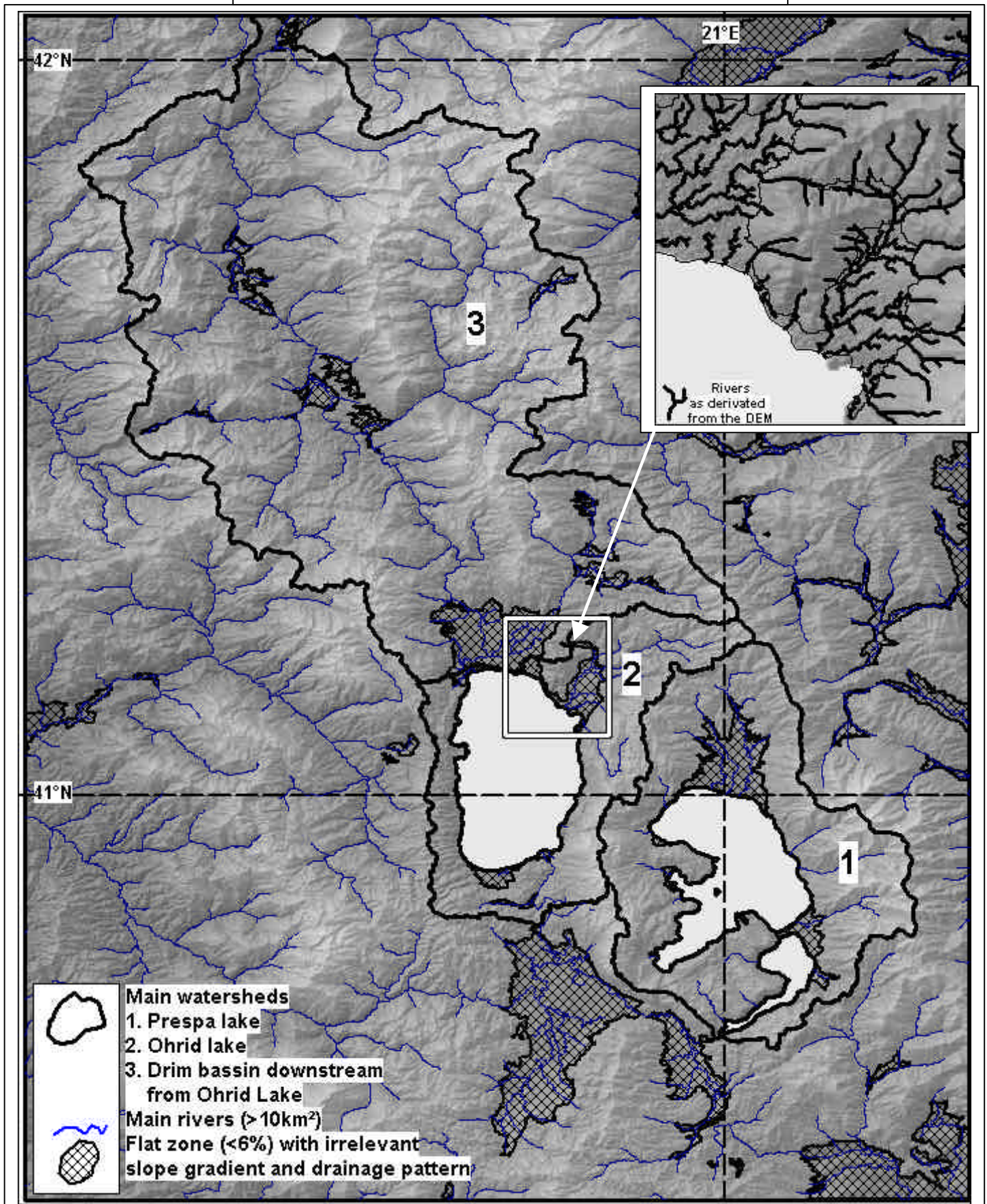


Figure 5: watershed and river networks as derived from DEM/SRTM over the Ohrid region



**Figure 6a : reverse side of tetradrachm coin
representing the pattern of major massifs of the
region of Ephesus**

(issued between 336 and 334 BC to pay the persian army)



**Figure 6b : same region as depicted by the
DEM/SRTM in 2004**



Figure 7 :
example of MAPAM processing
on the Gorenichka massif

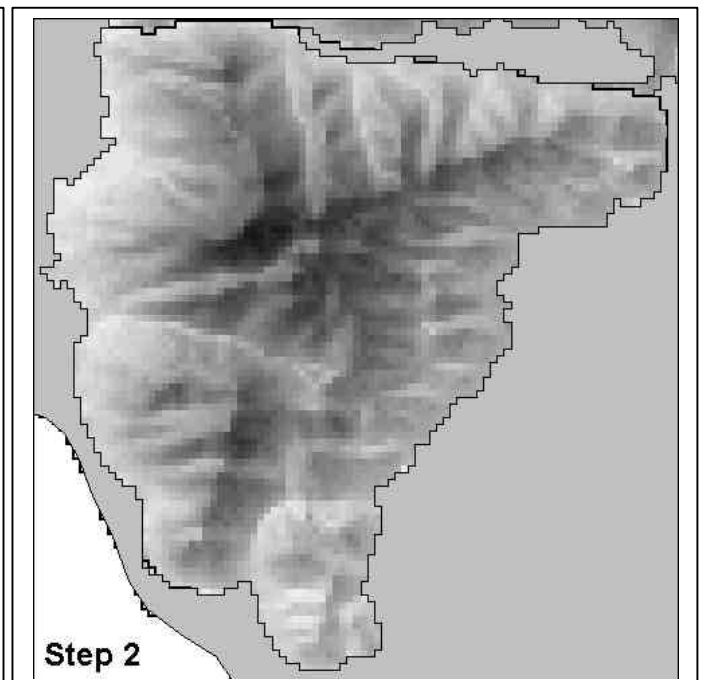
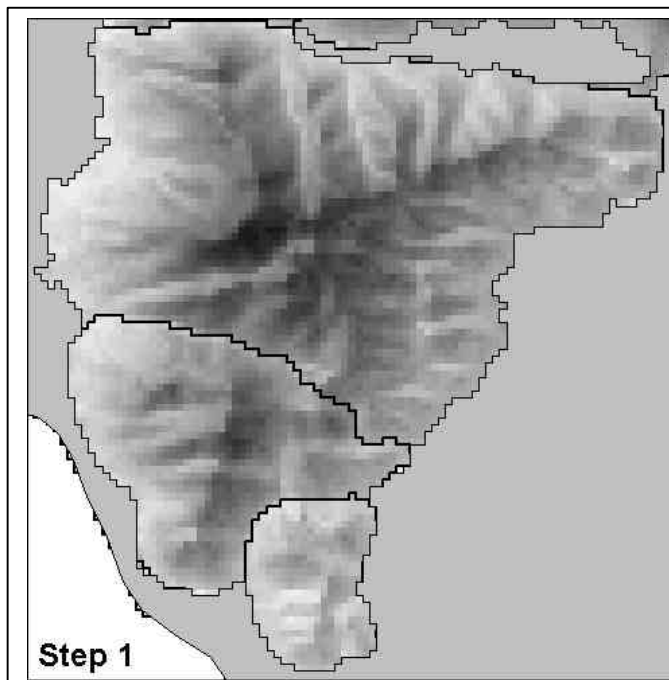
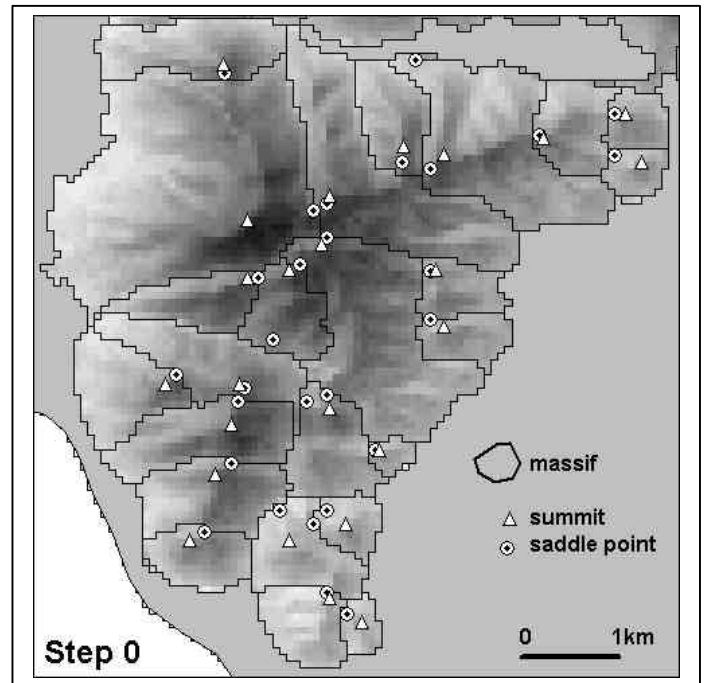
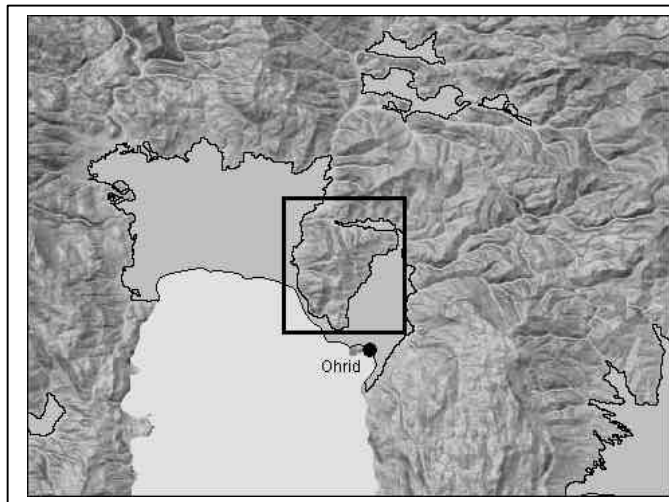


Figure 8 :
Evolution of landform indices
for Gorenichka massif
from step 0 to step 8
in the MAPAM process

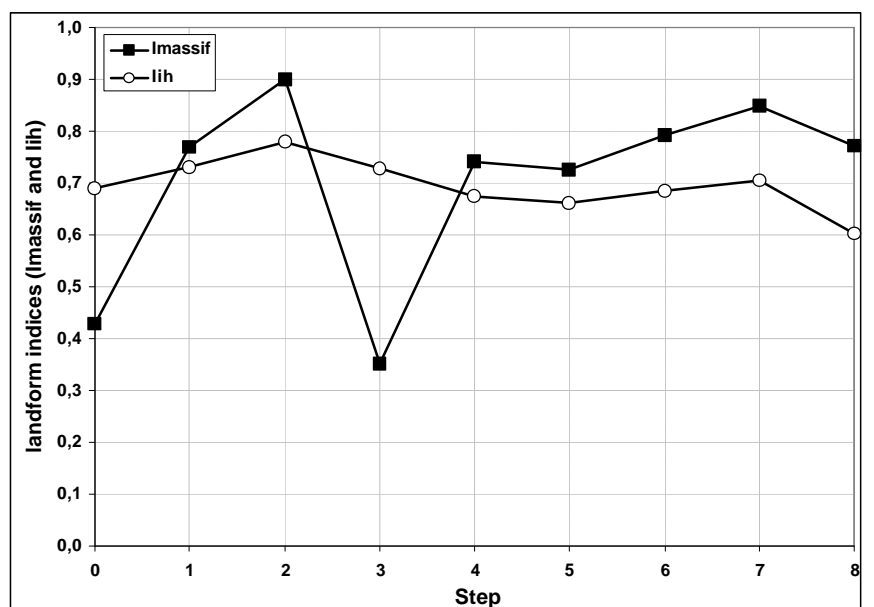


Figure 9 : directional variogram of the land surface over the Ohrid region

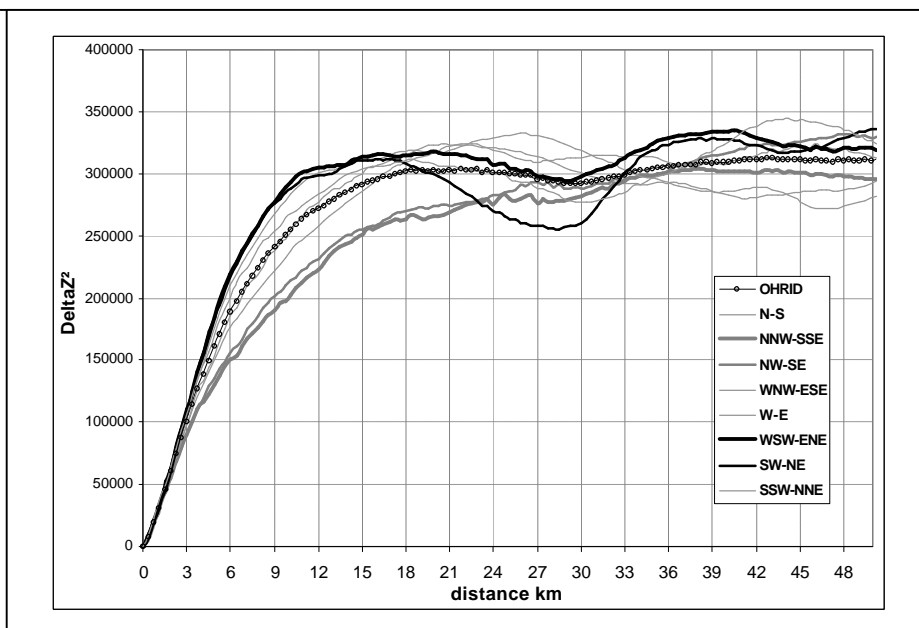


Figure 10 : average paving of landform according to the directional variogram

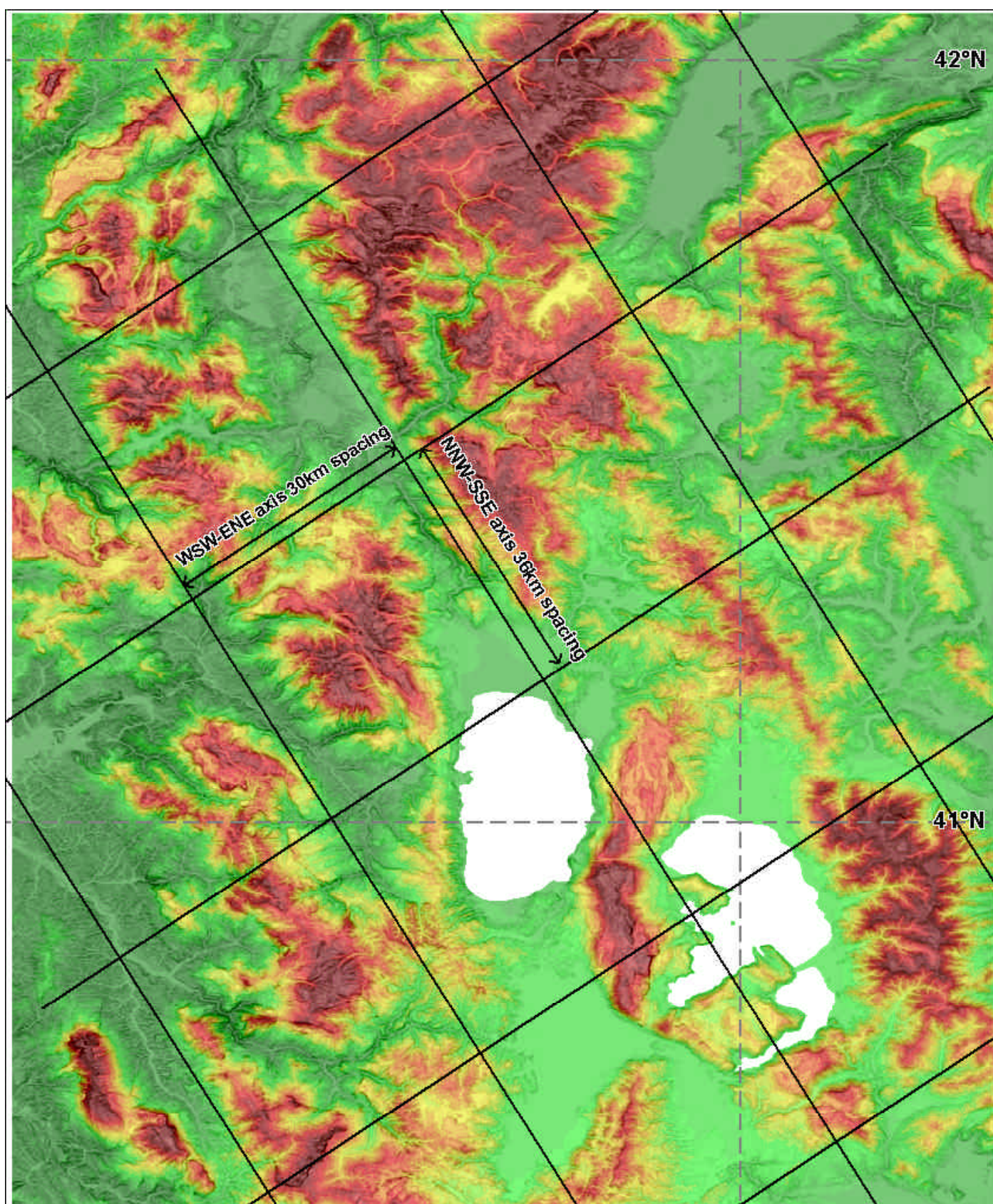


Figure 11 : average landform indices from step 0 to step 8

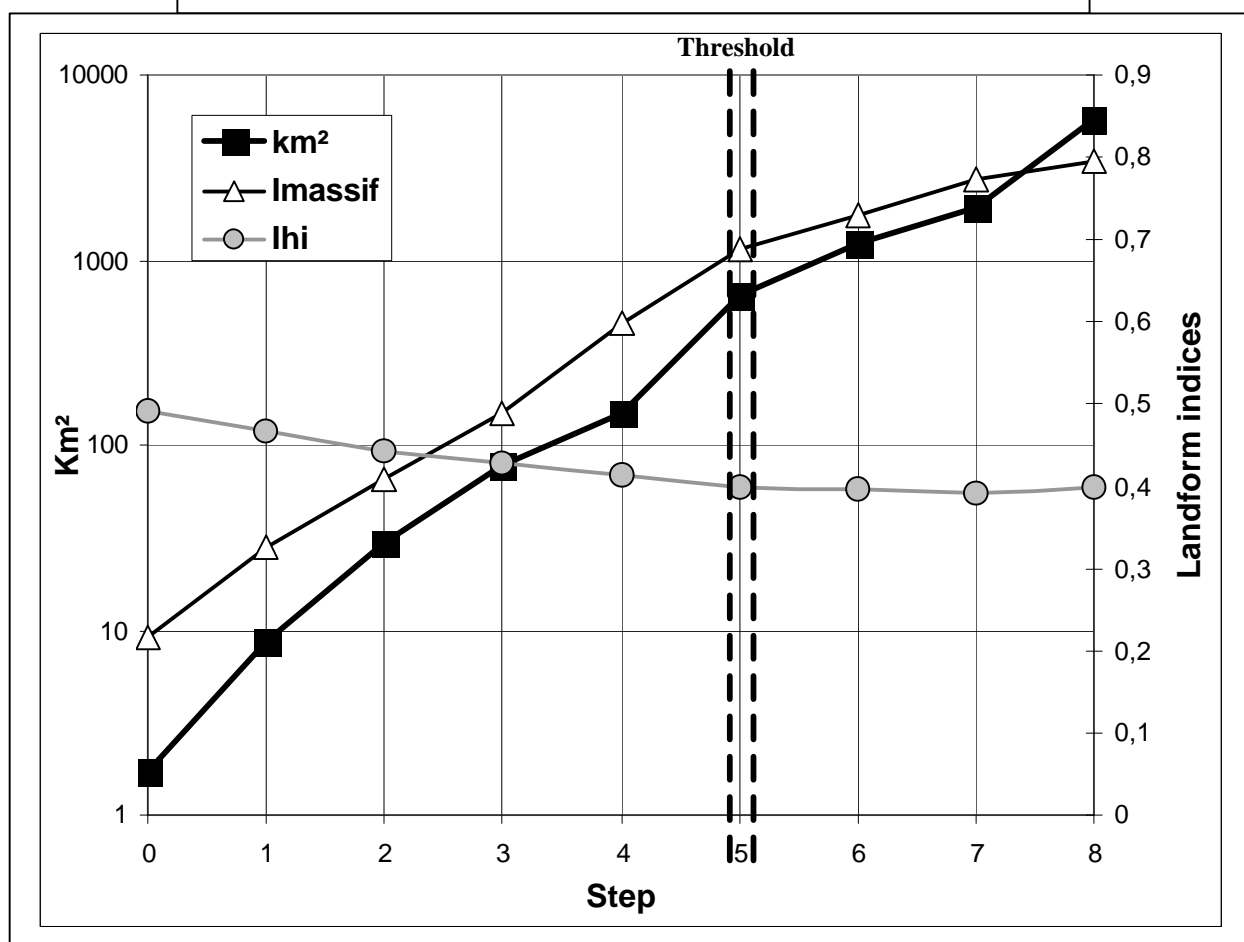


Figure 12 : pattern of massif partitioning from step 0 to step 5

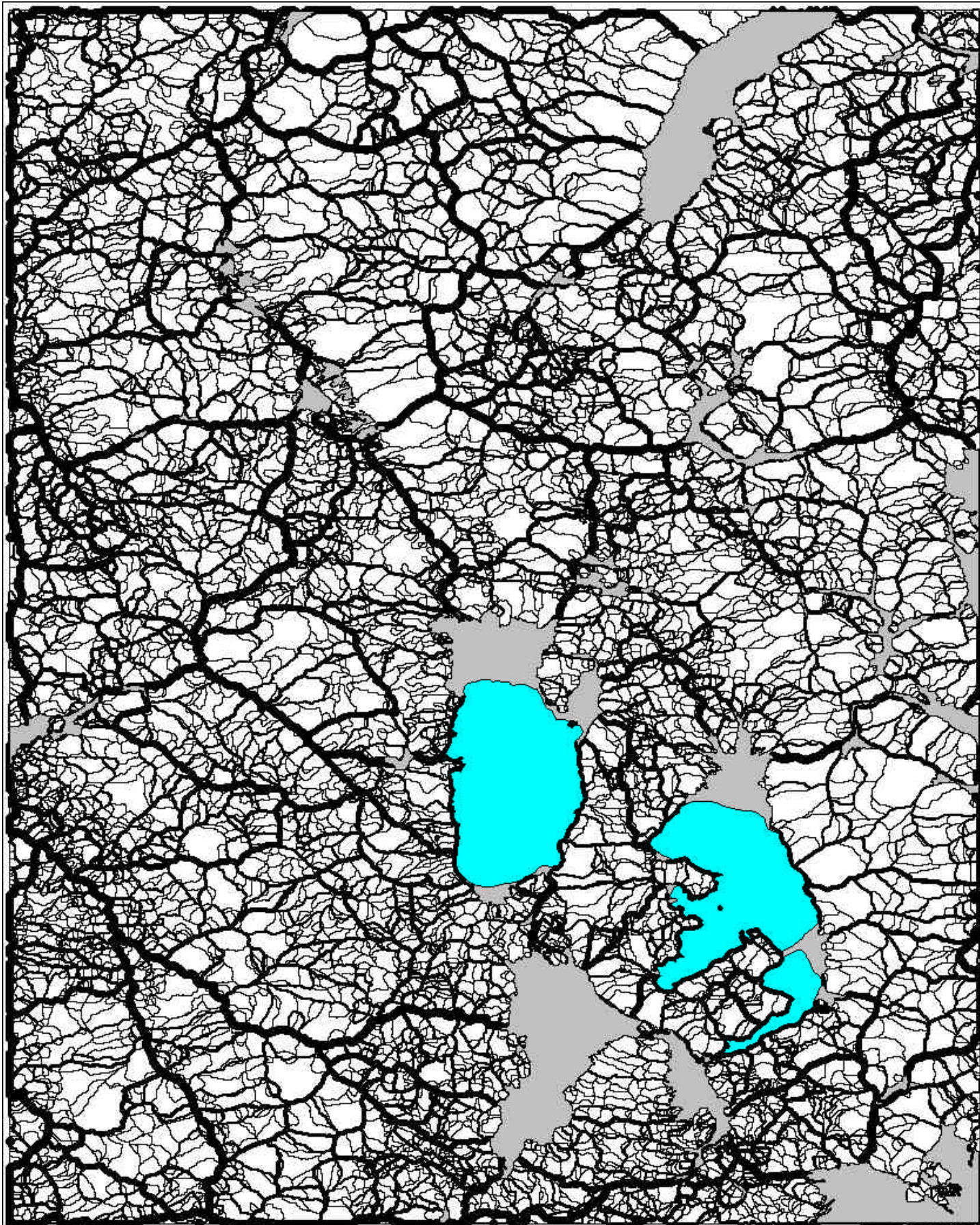


Figure 13 : well defined massifs overs the ohrid region

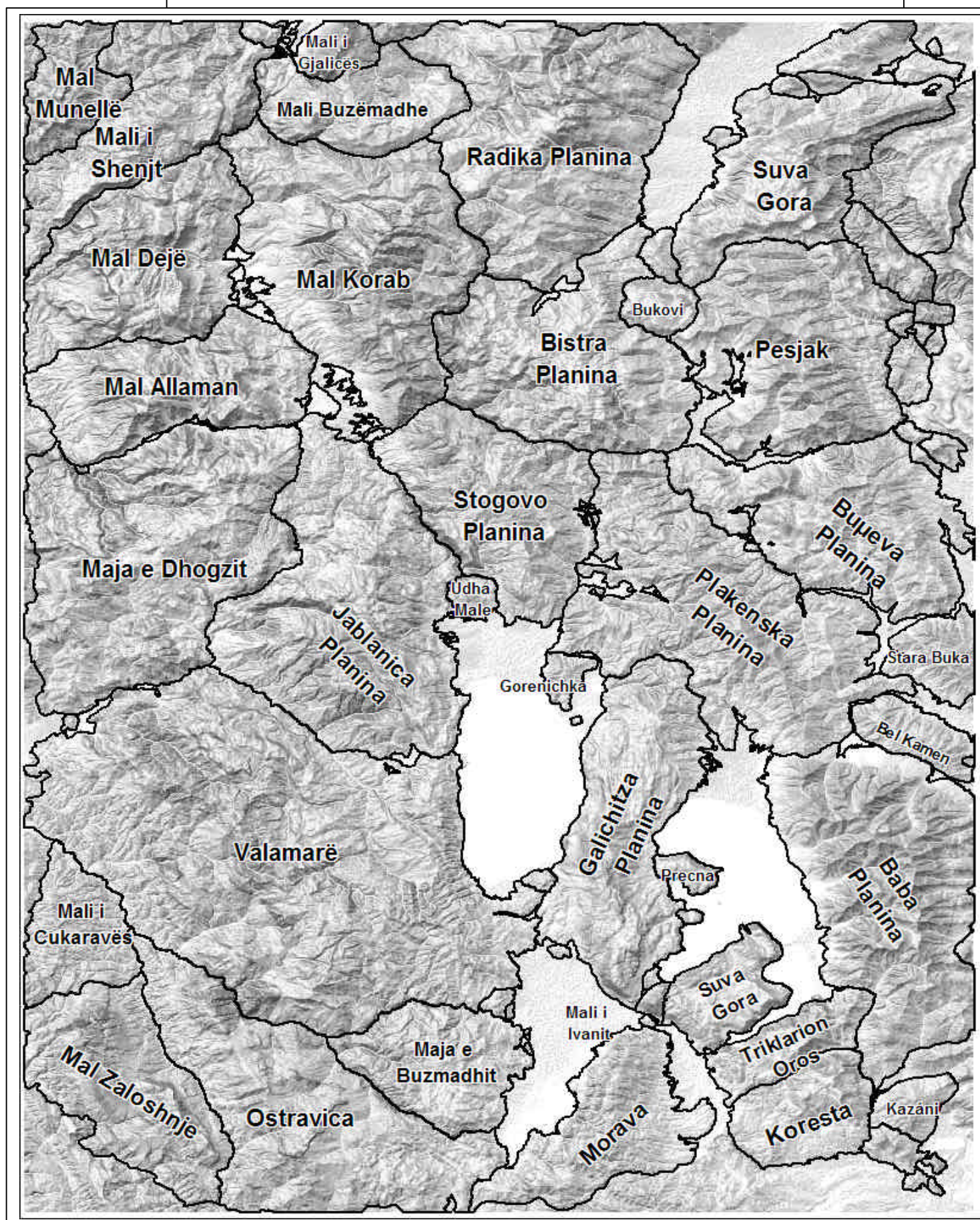


Figure 14 : geological maps of the Ohrid region and the calibration set of massifs

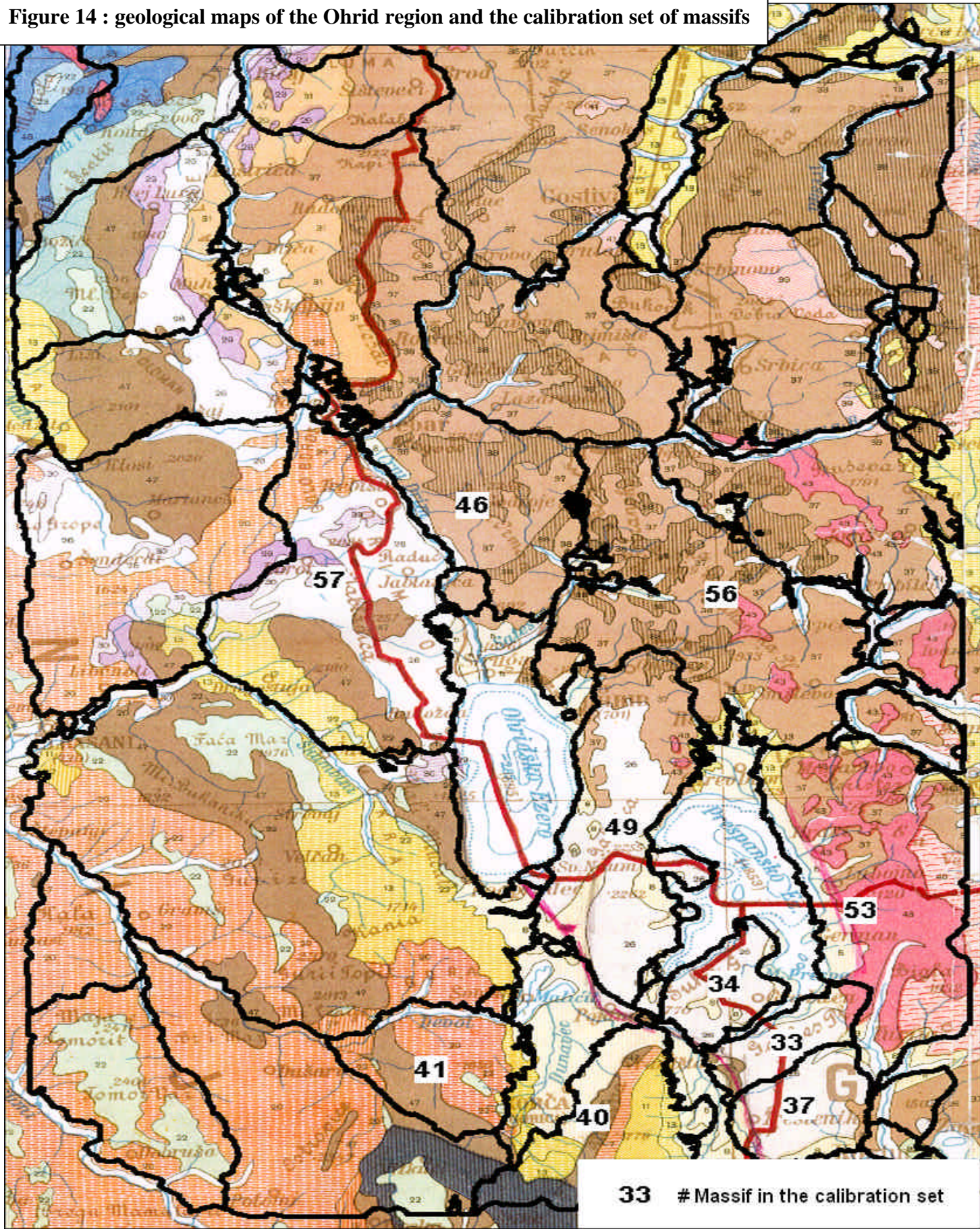


Figure 15 : Hillslope classification according to plan convexity versus profile convexity (adapted from Ruhe 1975)


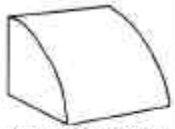


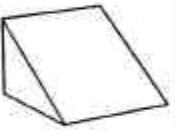




Profile convexity (Cprof)	Neutral	Cprof>0			
			Concave Convex (-+)	Neutral Convex (0+)	Convex Convex (++)
	Cprof=0				
		Concave Neutral (-0)	Neutral Neutral (00)	Convex Neutral (+0)	
	Cprof<0				
		Concave Concave (--)	Neutral Concave (0-)	Convex Concave (+-)	
Concave		Cplan<0	Cplan=0	Cplan>0	
		Concave	Neutral	Convex	
		Plan convexity (Cplan)			

Figure 16 : relationship between plan convexity and profile convexity on the Galichitza massif (#49) and computation of morphometrical signature criteria a_{global} , a_{crest} and a_{talweg}

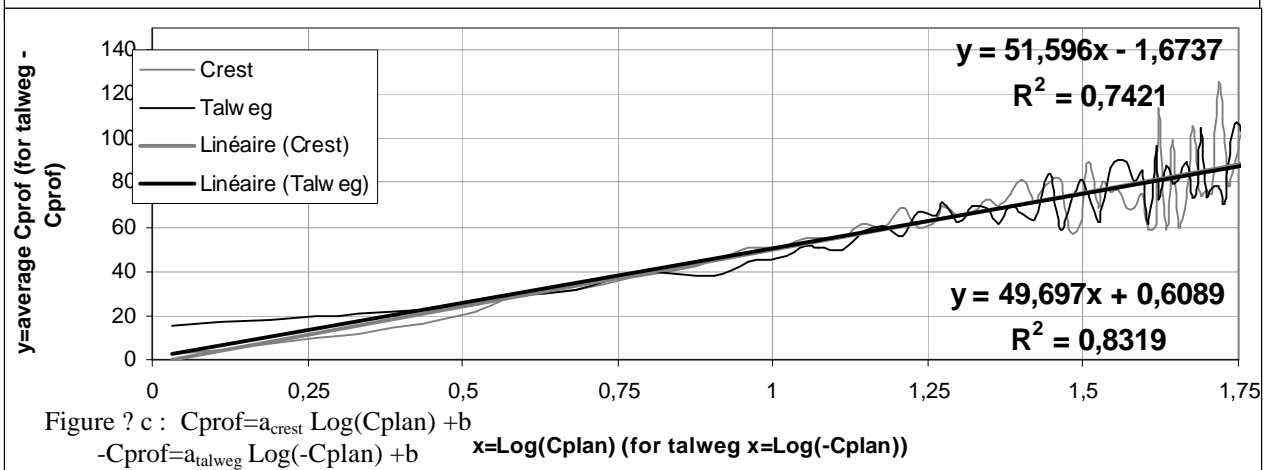
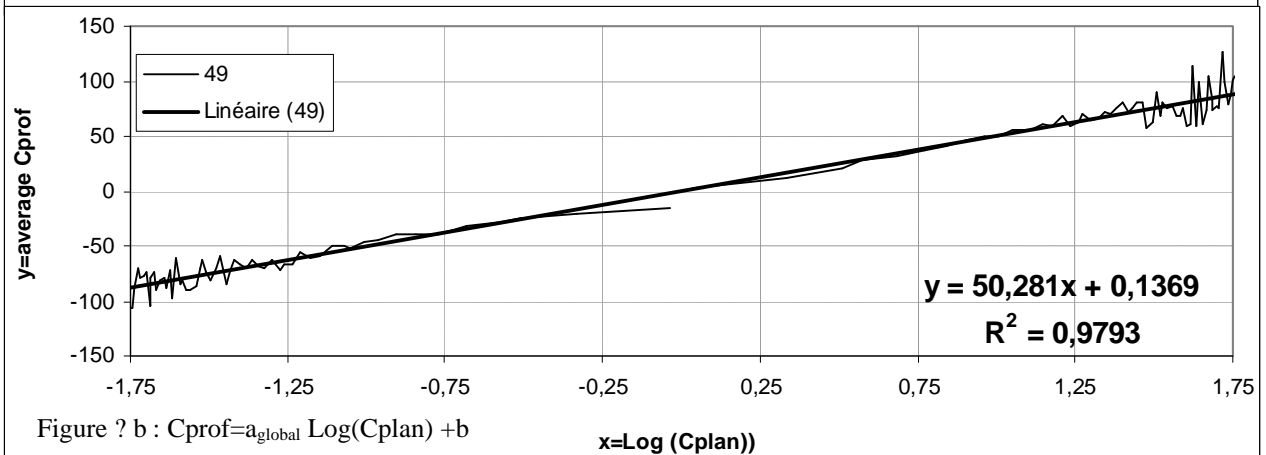
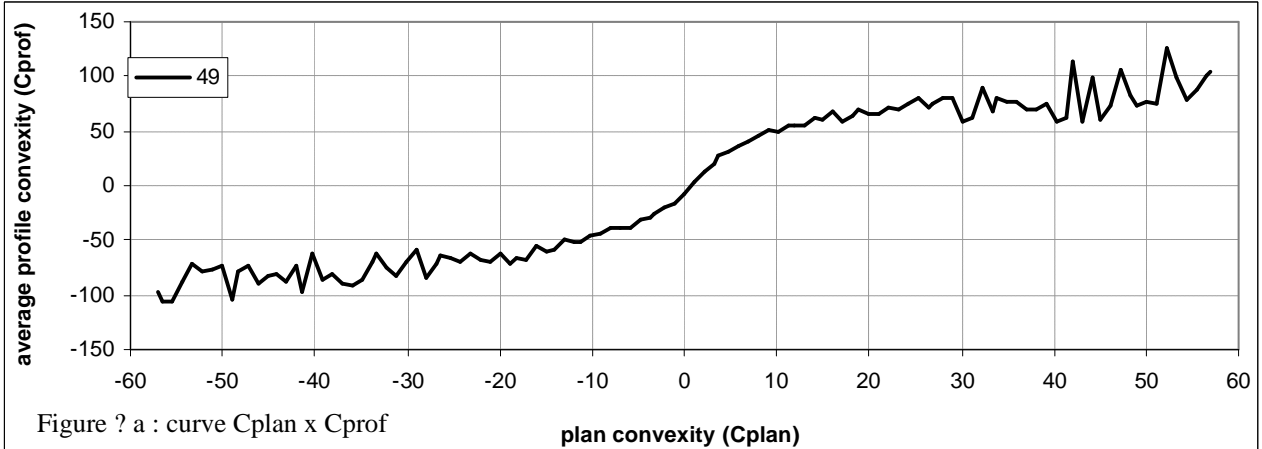


Figure 17 : diagnosis of karst geomorphometrical signature with the Score K criteria

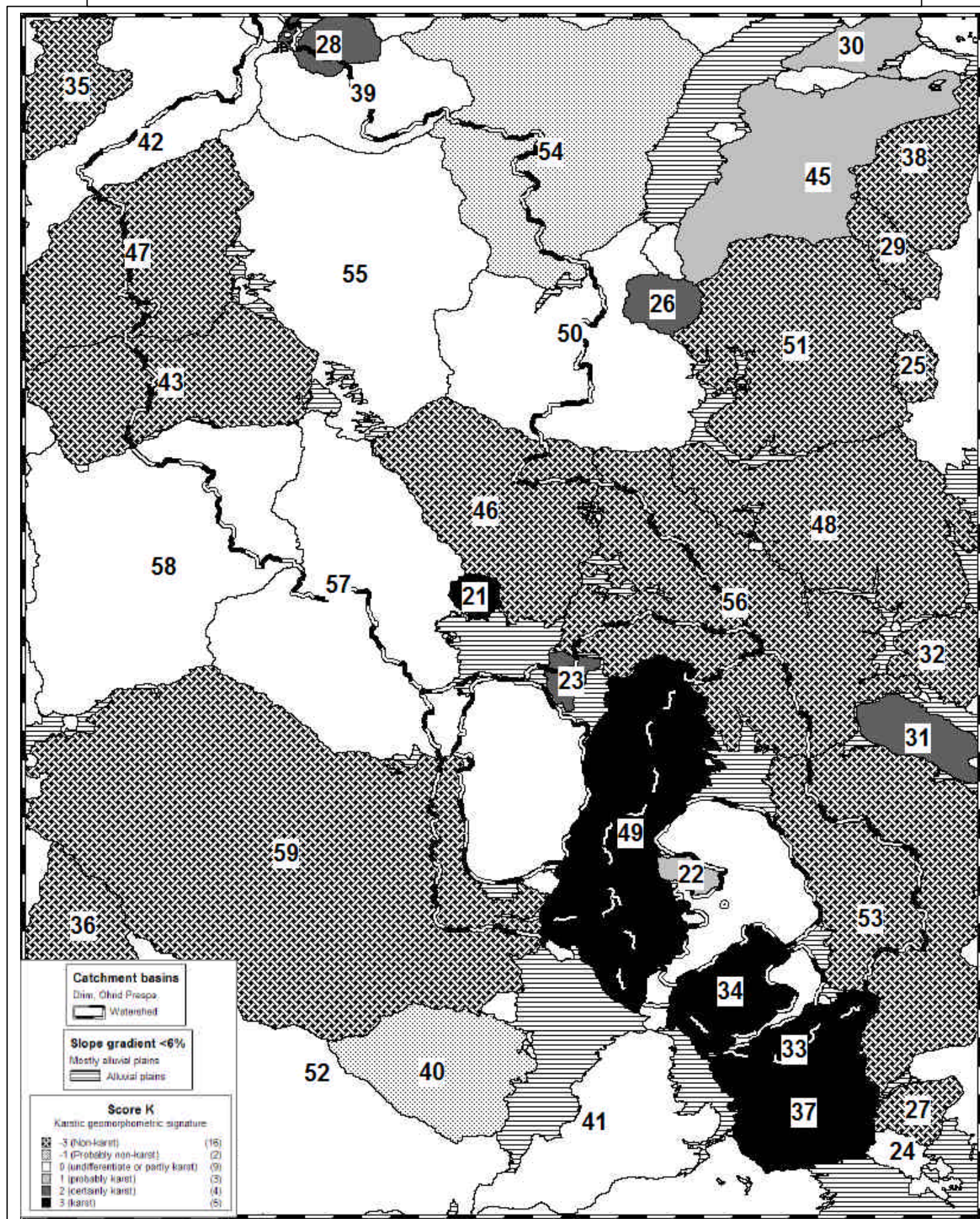


Figure 18 : Application of the MAPAM method over the Balkan peninsula



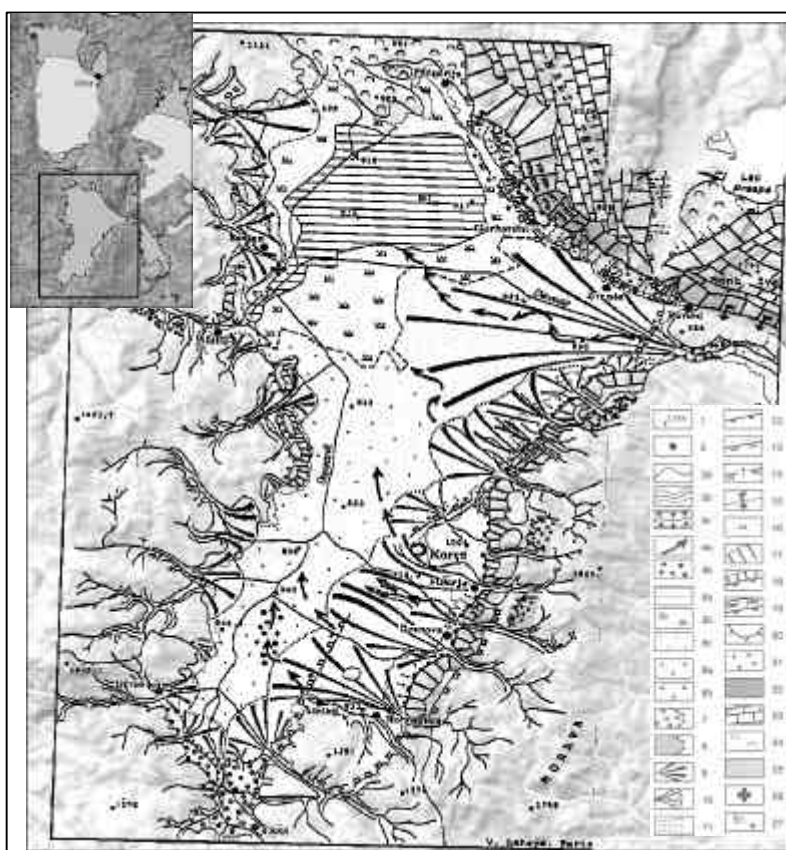


Figure 19a: The Korçë depression and related landforms at the foothills of surrounding massifs (Dufaure, 2003)

LEGEND

- 1 point coté
- 2 localité
- 3a thalweg à écoulement pérenne
- 3b thalweg encaissé
- 3c gorge épigénique
- 4a ancien cours abandonné
- 4b épandages grossiers associés
- 5a lac de Maliq en 1948
- 5b marécages associés en 1948
- 5c remblaiement alluvial récent
- 6a brèches anciennes et chaos de blocs
- 6b lobes d'éboulement quaternaires postérieurs associés aux tremblements de terre
- 7 terrasses alluviales du Pléistocène Moyen
- 8 formations rouges du Pléistocène Moyen
- 9 cônes d'épandages et glaciols holocènes
- 10 cônes bréchiqes du Pléistocène Récent
- 11 colluvions et blocs holocènes descendus des parois
- 12 ligne de faille à activité quaternaire avérée
- 13 ligne de faille sans preuve de rejeu récent
- 14 ligne de faille présumée
- 15 flexure
- 16 pendage local
- 17 escarpement à facette (versant régularisé)
- 18 escarpement de faille à facettes
- 19 escarpement de faille à murailles
- 20 abrupt monoclinal
- 21 dépôts alluviaux
- 22 ophiolithes
- 23 massif calcaire karstifié
- 24 collines pliocènes
- 25 molasse néogène
- 26 Tell de Sovjan

Figure 19b:
Same region processed with
DEM/SRTM: soil potential
saturation index
(SPSI, Beven method)

